Journal of Cleaner Production 234 (2019) 285–296

Contents lists available at ScienceDirect

Journal of Cleaner Production

journal homepage: www.elsevier.com/locate/jclepro

Optimization of parabolic through collector (PTC) with multi objective swarm optimization (MOPSO) and energy, exergy and economic analyses

M.A. Ehyaei [a, *], A. Ahmadi [b], M. El Haj Assad [c], Tariq Salameh [c]

[a] Department of Mechanical Engineering, Pardis Branch, Islamic Azad University, Pardis New City, Islamic Republic of Iran
[b] School of New Technologies, Iran University of Science & Technology, Islamic Republic of Iran
[c] Sustainable & Renewable Energy Engineering Department, University of Sharjah, United Arab Emirates

ARTICLE INFO

Article history:
Received 31 March 2019
Received in revised form
16 June 2019
Accepted 18 June 2019
Available online 22 June 2019

Handling editor: Prof. Jiri Jaromir Klemeš

Keywords:
Solar
PTC
Absorber
Exergy
Cost
MOPSO

ABSTRACT

The availability of reliable electricity and heat sources for community guarantees a better living environment in terms of education, healthcare and economy. Two main parameters should be considered in heat production which are the cost of this production and the performance of the devices used to produce this heat. In this work, a thermodynamic analysis based on energy and exergy analyses as well as economic analysis are presented to analyze the performance of parabolic trough solar collector (PTC). A multiobjective swarm optimization (MOPSO) technique is used to find out the maximum exergy efficiency and the minimum heat production cost of PTC. The optimum results show that the exergy efficiency, energy efficiency and heat cost are 29.22%, 35.55% and 0.0142 $/kWh. The effect of PTC geometrical parameters such as length, focal length, width and internal absorber diameter on the performance of PTC and heat production cost are investigated. Energy efficiencies of the system at different times during the day are calculated and they are in good agreement with the experimental results available in literature. The proposed system of PTC is located in Tehran, Iran.

1. Introduction

Solar energy is one of the abounded renewable energy resources distributed in the world. Utilization of solar energy can be used based on its application at low, intermediate and high temperature (Jebasingh and Herbert, 2016; Yousefi and Ehyaei, 2017).

One of these applications is Concentrated Solar Power plant (CSP). CSP depends on the reflected sun ray from the concentrator to the receiver in order to increase the temperature of the working fluid (Jebasingh and Herbert, 2016; Yousefi and Ehyaei, 2017).

There are two types of CSP which vary based on the shape of optical concentrator namely point or line focusing. Point focusing produces higher temperature than the line focusing and it requires two axis tacking. Both power tower and parabolic dish CSP are considered as point focusing, while Parabolic Trough (PT) and Fresnel CSP are considered as line focusing (Fuqiang et al., 2017).

Parabolic trough concentrated solar power (PTCSP) can be integrated easily with conventional power plant such as steam turbine (Rankine cycle) or gas turbine (Brayton cycle). This integration is carried out to achieve higher integrated system efficiency at low environmental impact t (Jebasingh and Herbert, 2016; Yousefi and Ehyaei, 2017).

There are many configurations of PTCSP used in power plants, these configurations vary based on many parameters such as type of integration, type of working fluid, thermal storage system, shape of receiver, types of tracking system and reflector, and receiver (absorber) materials (Ehyaei et al., 2019; Fernández-García et al., 2010).

Due to the high dependency of PTCSP performance on the above mentioned parameters it is not easy to find out the best performance of PTCSP without helping of optimization methods (Fernández-García et al., 2010).

There are many optimization techniques that have been used recently for optimization purposes, which are known as Artificial Intelligence (AI). These optimization methods are used to find the maximum delivered power from any energy system under some constrains. These constraints are related to the previously

* Corresponding author.
E-mail address: aliehyaei@yahoo.com (M.A. Ehyaei).

https://doi.org/10.1016/j.jclepro.2019.06.210
0959-6526/

mentioned parameters and operating conditions of PTCSP. Furthermore, these optimization techniques help the energy system to operate at low level cost of energy (LCOE) and low Green House Gas Emissions (GHGE) (Ehyaei and Rosen, 2019; S. Aravindan, 2018; Sadeghzadeh, H et al., 2015; Shamoushaki et al., 2017b).

Optimization problems existing in real world are multi-objective problems which means optimal solutions should be obtained simultaneously when considering multi conflicting objectives. Among these techniques are the multi-objective optimization problems (MOPSO) and Artificial Bee Colony (ABC). Multi Objective Optimization or vector optimization is used for the problem that has a set of objectives instead of single objective. Multi Objective Optimization Problem (MOP) consists of two types: (1) linear and nonlinear (2) convex and non-convex. Linear MOP is considered when all objective functions and constraints are linear, whereas nonlinear MOP is considered when any of the objective or constraint function is nonlinear. Convex MOP is considered when the objective functions are convex and feasible region is convex and non-convex MOP is considered when the objective functions and feasible region are non-convex (Ghasemian and Ehyaei, 2018; S. Aravindan, 2018; Sadeghzadeh et al., 2015a,b; Shamoushaki et al., 2017a).

There ae two popular AI techniques for solving MOPs, these are Evolutionary Approaches (EAs) such as Vector Evaluated Genetic Algorithm (VEGA) and Particle Swarm Optimization (PSO). Multi objective Swarm Particle Optimization (MOSPO) is derived from Particle Swarm Optimization (PSO) domain after Swarm Intelligence (SI) techniques exist (Ab Wahab et al., 2015; Asgari and Ehyaei, 2015; Yazdi et al., 2015).

Artificial neural network (ANN) model have been used to predict LCOE, annual power generation and capacity factor for parabolic trough solar thermal power plants (PTSTPPS) integrated with energy storage (Boukelia et al., 2017) where thermic oil and molten salt as primary heat transfer fluids in the solar field were used.

Other optimization methods such as least squares support vector machine (LSSVM) was developed to model solar collector system in PT (Liu et al., 2012) where the feasibility and efficiency of the LSSVM method were evaluated experimentally and numerically for two solar collector systems. Memetic algorithm was used to study the influence of objective functions for life cycle savings, LCOE and payback time on optimal design point location in PTSP (Silva et al., 2014) where a multi-objective optimization approach was used to design the PT from a multi-economic criteria point of view.

A multi-parameter optimization of PTS receiver based on genetic algorithm has been applied (Guo and Huai, 2016) where both thermal and exergy efficiency were taken as objective function to study the thermal behavior of PTS receiver. Again ANN models based on the feed-forward back-propagation learning algorithm with three different variants were used to predict the annual power and LCOE for PTSTPP (Boukelia et al., 2016).

Hybrid optimization algorithm method including genetic algorithm and sequential quadratic programming (SQP) was used in non-convex and non-linear optimization process for thermal analysis in a solar PT collector based on Nano fluid (Shirmohammadi et al., 2015; Zadeh et al., 2015).

Optimization of two PTSTPP in Algeria was performed (Boukelia et al., 2015) for which the optimization was used based on the objective of maximizing the annual energy yield and minimizing the LCOE. Solar multiple (SM) and full load hours of thermal energy system parameters were implemented during the optimization process. Solar multiple optimization has been extensively used by many researchers (Boukelia et al., 2015; Montes et al., 2009a, 2009b).

Artificial Bee Colony (ABC) is another technique used for optimization purposes. Compared to PSO technique, Artificial Bee Colony (ABC) algorithm delivers more accurate optimization results than PSO, but it needs more time for convergence. On the other hand, PSO is faster than ABC; but its accuracy is relatively lower than ABC (Kulkarni and Desai, 2016).

PSO has many advantages such as providing simple calculation, less dependency of a set of initial points, fast convergence, easy to implement and small impact of parameters to the solution. As a result of these advantages, MOPSO technique is implemented in this study remembering that it is just a tool to determine the best performance of the proposed energy system. Hence, our main interest is in obtaining the optimum values of exergy efficiency, energy efficiency and heat cost (Kulkarni and Desai, 2016).

This study proposes, for the first time, the combined three analyses namely energy, exergy and economic analyses using MOPSO algorithm to obtain the best possible performance of PTC at the cheapest heat production cost. Hence, the aim of this work is to determine the energy, exergy efficiencies as well as the heat production cost of PTC system located in Tehran, Iran. The novelty of this work is as follows:

- Considering energy, exergy and economic analyses in optimization of PTC
- Optimization of a PTC with MOPSO algorithm
- Selection the best geometric specification and working fluid mass flow rate to improve heat gain, energy and exergy efficiencies and heat produced cost by PTC
- Sensitivity analysis of optimized parameters
- Extension of study by optimization of a PTC with multi-objective shuffled frog-leaping algorithm
- Comparison optimized values of two optimization algorithms

2. Mathematical modeling

2.1. Energy modeling

The schematic diagram of the system as well as the side views of PTC are shown in Fig. 1.

The solar time can be obtained as (Duffie, 1991):

$$T_{ls} = T_l + 4\,(L_{loc} - L_{st}) + E \tag{1}$$

where T_s and T_{ls} are the solar time and local time, respectively, L_{st} is the local standard time meridian and L_{loc} is the site longitude, and E is the equation of time which is calculated by the (Duffie, 1991):

$$E = 229.2\,(0.000075 + 0.001868\text{Cos}\,\beta - 0.032077\text{Sin}\,\beta - 0.014615\,\text{Cos}\,2\beta - 0.04089\,\text{Sin}\,2\beta) \tag{2}$$

where $\beta = \frac{360(n-1)}{365}$ (1st of January n = 1).

The sunset hour angle for horizontal surface is expressed as (Duffie, 1991):

$$\omega = \cos^{-1}(-\tan\varphi\,\tan\delta) \tag{3}$$

where φ and δ are the latitude and deflection angle respectively.

The deflection angle can be found from δ (Sukhatme and Sukhatme, 1996):

$$\delta = 23.45\sin\left(\frac{360(284+n)}{365}\right) \tag{4}$$

The direct normal irradiance (DNI) is given by (Sukhatme and

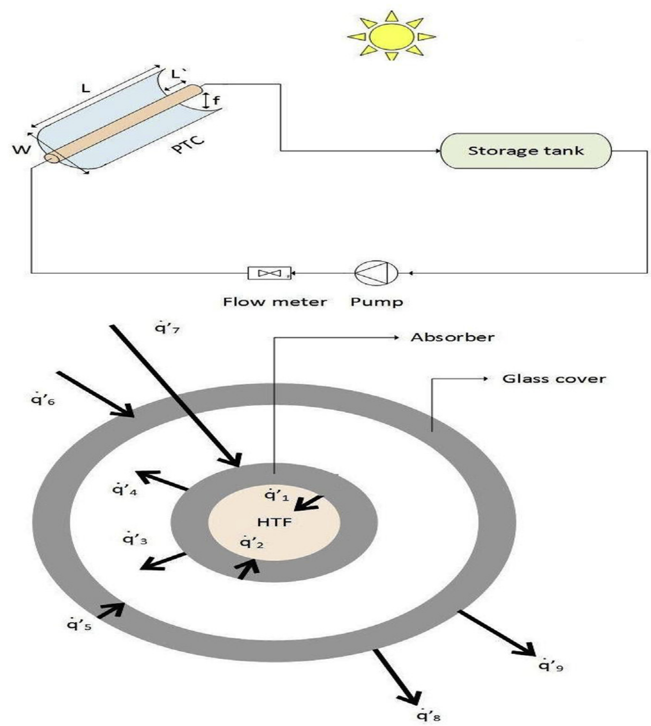

Fig. 1. Schematic diagrams of the system and PTC.

Sukhatme, 1996):

$$DNI = A\cos\theta_z \exp\left(\frac{-B}{\cos\theta_Z}\right) \tag{5}$$

where A and B are constants given in Ref (Sukhatme and Sukhatme, 1996), and θ_Z is the Zenith angle.

PTC optical efficiency is defined as (Hachicha et al., 2013):

$$\eta_{opt} = \rho\tau\alpha\gamma KL' \tag{6}$$

where ρ is the mirror reflectance, τ is the glass cover transmittance, α is the receiver absorptance, γ is the intercept factor, K is the angle of incidence incident angle modifier and ξ is the end loss factor. γ is defined as the fraction of reflected radiation in the absorber to the total reflected radiation by the collector and includes all the optical errors (Forristall, 2003; Güven and Bannerot, 1986; Khaled, 2012). In this work, the intercept factor is taken as 0.92 which is an acceptable value in literature.

The end loss factor is expressed as (Alfellag, 2014; Vasquez Padilla, 2011):

$$L' = 1 - \frac{f}{L}\,tg\theta_z \tag{7}$$

where f is the focal length and L is the collector length of collector.

The energy balance equations for cross-section views shown in Fig. 1 are as follows (Ehyaei et al., 2019):

$$\dot{q}'_1 = \dot{q}'_2 \tag{8}$$

$$\dot{q}'_7 = \dot{q}'_2 + \dot{q}'_3 + \dot{q}'_4 \tag{9}$$

$$\dot{q}'_5 = \dot{q}'_3 + \dot{q}'_4 \tag{10}$$

$$\dot{q}'_5 + \dot{q}'_6 = \dot{q}'_8 + \dot{q}'_9 = \dot{q}'_{loss} \tag{11}$$

The PTC outlet temperature of PTC is (Coccia et al., 2012; Forristall, 2003):

$$T_{i+1} = T_{i-1} + \frac{1}{(\dot{m}c_p)\left(\dot{q}'_6 + \dot{q}'_7 - \dot{q}'_8 - \dot{q}'_9\right)\Delta L} \tag{12}$$

where T is temperature, $\dot{m}$ is the mass flow rate, ΔL is the section length and c_p is the specific heat.

Nusselt numbers for turbulent and laminar pipe flow are, respectively (Bergman et al., 2011; Gnielinski, 1976):

$$NuD = \frac{\left(\frac{f}{8}\right)(Re - 1000)Pr}{1 + 12.7\sqrt{\frac{f}{8}}\left(Pr^{\frac{2}{3}} - 1\right)}\left(\frac{Pr}{Prw}\right)^{0.11} \quad 2300 \le Re \le 10^6 \tag{13}$$

$$Nu_D = 4.36 \quad Re < 2300$$

Where f is the friction coefficient, Re is the Reynolds number, Pr is the Prandtl number and Pr_w is the Prandtl number at the wall.

The convection heat transfer coefficient in the evacuated space between the absorber and glass is expressed as (Kalogirou, 2012; Ratzel et al., 1979):

$$h = \frac{k}{\frac{D_{outer-absorber}}{2\ln\left(\frac{D_{inner-glass}}{D_{outer-absorber}}\right)} + b\lambda\left(\frac{D_{outer-absorber}}{D_{inner-glass}} + 1\right)} \tag{14}$$

where D is the diameter, k is the thermal conductivity, b is the interaction parameter which is obtained from Ref (Kalogirou, 2012; Ratzel et al., 1979) and λ is the mean free path of molecules collisions.

The radiation heat transfer rate in the evacuated space is (Yunus and Afshin, 2011):

$$\dot{q}'_{rad,\ outer\ absorber-innerglass} = \frac{\pi\sigma D_{outer-absorber}\left(T^4_{outer-absorber} - T^4_{inner-glass}\right)}{\frac{1}{\varepsilon_{outer-absorber}} + \frac{(1-\varepsilon_{inner-glass})D_{outer-absorber}}{\varepsilon_{inner-glass}\,D_{inner-glass}}} \tag{15}$$

where ε is the emissivity and σ is the Stefan- Boltzmann constant ($5.672^{*}\ 10^{-8}\ \frac{W}{m^2K^4}$).

.The Nusselt number of the ambient air in the presence of wind speed surrounding the outer glass is obtained as (Rathore and Kapuno, 2011):

$$Nu_{D,\ outer-glass} = C\,Re^m_{outer-glass}Pr^n_a\left(\frac{Pr_a}{Pr_{outer-glass}}\right)^{\frac{1}{4}} \tag{16}$$

where C, m, and n are constants determined from Ref (Rathore and Kapuno, 2011).Subscripts a and outer-glass mean that Prandtl number should be calculated at these temperatures, respectively.

The system energy efficiency is obtained as (Okonkwo et al., 2018):

$$\text{Energy efficiency} = \frac{\dot{q}_u - \dot{W}_{pump}}{DNI * A} \quad (17)$$

Where the pump work is $\dot{W}_p$, I_t is the solar radiation and A is the collector surface area. The useful heat gain $\dot{q}_u$ by the PTC is

$$\dot{q}_u = \dot{m}\, cp\, (T_o - T_i) \quad (18)$$

where $\dot{m}$ is the mass flow rate of HTF. T_o ($^\circ C$) and T_i ($^\circ C$) are the outlet and inlet HTF temperatures, respectively.

2.2. Exergy modeling

Neglecting the kinetic and potential exergies, and considering that the chemical exergy is constant through the flow, then the specific exergy can be only written in terms of physical exergy as (Bejan, 2016; Padilla et al., 2014; Petela, 1964):

$$e_x = (h - h_0) - T_0(s - s_0) \quad (19)$$

where h (kJ/kg) is the enthalpy and s (kJ/kgK) is specific entropy. The subscript 0 represents the dead state (1 atm, 20°C).

Exergy destruction rate can be written as (Bejan, 2016; Padilla et al., 2014; Petela, 1964):

$$\dot{E}_D = (\dot{m}(ex_i - ex_o) + A * DNI \left(1 - \frac{4}{3}\left(\frac{T_{amb}}{T_{sun}}\right) + \frac{1}{3}\left(\frac{T_{amb}}{T_{sun}}\right)^4\right) + \dot{q}'_{loss}L + \dot{W}_{pump}\Bigg) \quad (20)$$

where the sun temperature T_{sun} is taken as 5800 K, ex_i and ex_o are the specific exergies of the HTF at the inlet and outlet, respectively.

Exergy efficiency can be calculated by (Bejan, 2016; Padilla et al., 2014; Petela, 1964):

$$\text{Exergy efficiency} = \frac{\dot{m}(ex_i - ex_o) - \dot{q}'_{loss}L - \dot{W}_{pump}}{A * DNI \left(1 - \frac{4}{3}\left(\frac{T_{amb}}{T_{sun}}\right) + \frac{1}{3}\left(\frac{T_{amb}}{T_{sun}}\right)^4\right)} \quad (21)$$

2.3. Economic modeling

The heat production cost of PTC is given by (Frangopoulos, 1987; Horngren et al., 2010):

$$C_H = \frac{C_I \frac{(1+i)^n}{(1+i)^n - 1} + C_{OM}}{\dot{q}_u} \quad (22)$$

where C ($) is the cost. Subscripts H, I and OM mean heat, initial and operation, and maintenance. i is the interest rate which is equal to 2% and n is a number of years.

The purchase costs of the proposed system components are given in Table 1 (Palenzuela et al., 2015) (Silveira and Tuna, 2003).

3. Optimization algorithms

Generally, optimization deals with finding a maximum or minimum for one and more objective functions which are function of single or multi variables to satisfy some constraints. In many engineering and real life cases, the optimization problems are so complex and they cannot be solved by traditional optimization methods. This problem is more complex when multi criteria or multi objective optimization are involved. So heuristic methods are more appropriate for this kind of problem, especially when the objective functions are non-linear, discontinues and non-differentiable functions (Hojjati et al., 2018).

Table 1
The purchase cost of system components.

No.	Component	Unit	Purchase cost	Ref.
1	Solar collector	$\$/m^2$	148	Palenzuela et al. (2015)
2	Working fluid (water)	$\$/m^2$	4	Palenzuela et al. (2015)
3	Storage tank	$\$/m^2$	27	Palenzuela et al. (2015)
4	Pump	$	$3540(\dot{W}_p^0)^{0.71}$	Silveira and Tuna (2003)

The mathematical form for optimization problems is given as follow (Han et al., 2018):

$$\text{Min/Max}\ F_n(X) = [f_1(X) ؛ f_2(X) ؛ \ \text{و}\ f_m(X)]^T \sqrt{b^2 - 4ac} \quad (23)$$

Subject to $g_j(X) \le 0$ for $j = 1, 2, \ldots, J$ $h_k(X) = 0$ for $k = 1, 2, \ldots, K$ $X^L \le X \le X^U$ where X is the multi-variable vector with n dimension $X(x_1, x_2, \ldots, x_n)$ and m represents the number of the objective functions. For m equals to 1, the optimization problem is single objective, otherwise the problem is multi-objective function. Also, L and U stand for lower and upper limit of vector X in search space, respectively. Several non-traditional solutions based on search methods can be applied for this problems.

3.1. Particle swarm optimization (PSO)

Evolutionary algorithms (EA) have been used for solving simple and complex problems with single and multi-objective functions for many years. One of the most recent evolutionary algorithms is the particle swarm optimization (PSO). PSO algorithm is a stochastic search method that is a powerful technique to solve complex problems at which other conventional methods fail to work (DASHENG, 2009).

The Particle swarm optimization (PSO) method is a comparatively new, innovative search method that is based on group behavior of birds, insects and fish schools. Like evolutionary algorithms, PSO algorithm is a population base where the population of a potential solution is called swarm and each individual of solution (population) within swarm is called a particle.

Each swarm initially is located at random locations in the multi-dimensional search space. For each particle, two parameters of position and velocity vector are assumed. Each particle can move randomly in a design space and can remember the best position in term of the food source or objective function value. Then, all particles are communicated information and good position to each other and they individually chose best position and velocity toward a best position received by the folk (Alvarez-Benitez et al., 2005; Rao, 2009; Reyes-Sierra and Coello, 2006).

Consider a search space with d dimension and the space vector and velocity vector for the i^{th} particle are given with $X_i(x_{i1}, x_{i2}, \ldots, x_{id})$ and V_i $(v_{i1}, v_{i2}, \ldots, v_{id})$ respectively. The P_i $(p_{i1}\ p_{i2}, \ldots, p_{id})$ stores the position coordinates corresponding to the best individual performance of the particle and it is called pbest. The best position obtained by the swarm is denoted as g $(g_1, g_2, , g_d)$ and it is called *gbest*. The position and velocity of each particle is updated toward the high or low value of objective function in maximization or minimization case respectively (Alvarez-Benitez et al., 2005; Rao, 2009; Reyes-Sierra and Coello, 2006).

The new position and new velocity of the particle are governed by the following equations (Alvarez-Benitez et al., 2005; Rao, 2009;

Reyes-Sierra and Coello, 2006):

$$V_i^{t+1} = wV_i^t + C_1 r_1 \left(x_{pbest} - X_i^t\right) + C_2 r_2 \left(x_{gbest} - X_i^t\right) \tag{24}$$

$$X_i^{t+1} = X_i^t + V_i^{t+1} \tag{25}$$

Where, w is an inertia weight, C_1 is a cognitive acceleration coefficient, $C_2$is a social acceleration coefficient, r_1 and r_2 are random numbers between [0, 1], x_{pbest} is the personal best of the particle, x_{gbest} is the global best of the particle in the swarm. Also, X_i^t and V_i^t are the current position and velocity of i^{th} particle at iteration t respectively and X_i^{t+1} and $V_i^{t+1}$are position and velocity vector of the i^{th} particle at iteration $t+1$ (Hosseini et al., 2015; Lalwani et al., 2013; Tripathi et al., 2007). Fig. 2 shows the flowchart for PSO algorithm (Tarique and Gabbar, 2013).

3.2. Multi-objective particle swarm optimization (MOPSO)

In PSO algorithm, there is just one objective function alongside with equality and inequality constraints. However, in multi-objective particle swarm optimization (MOPSO) algorithm, there are several objective functions which always conflicting with each other. The procedure of solution is same as before. Fig. 3 shows the flowchart solution for dominate solution (Kusiak and Xu, 2012) (El-Gammal and El-Samahy, 2009).

The performance of various Swarm Intelligence (SI) including Particle Swarm Optimization (PSO), Genetic algorithm (GA), Ant Colony Optimization (ACO), Differential Evolution (DE), Artificial Bee Colony (ABC) for about thirty benchmarks functions by using MATLAB have been performed. These benchmarks cover different range of objective function such as unimodal, multimodal, separate-able and in-separate-able function for different domains. The performance of these algorithm based on these benchmarks are evaluated. The results indicated the superiority of DE with the ability to outperform or perform equally to the best algorithm in 24 out of 30 functions. PSO is the second best approach that outperformed or performed equally to the best algorithm in 18 out of 30 functions and follows by GA with 14 out of 30 (Ab Wahab et al., 2015).

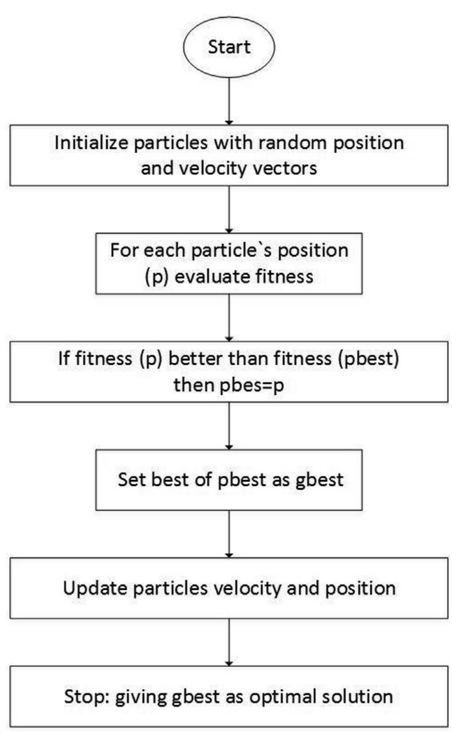

Fig. 2. Particle Swarm Optimization algorithm.

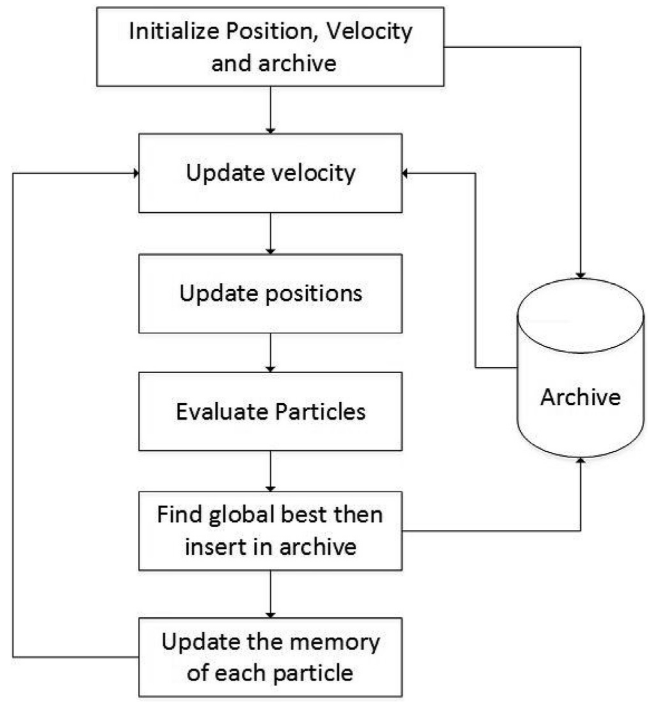

Fig. 3. Multi objective particle swarm optimization (MOPSO).

In comparison of ability of PSO and GA algorithm for problem solving, PSO is often refereed to outperformed over GA. It means, when these two algorithm are applied to various problems, PSO has better quality and faster performance relative to GA. Although PSO and GA share many similarities, but PSO has no evolution operators such as crossover and mutation in GA and potential solutions fly through the problem space by following the current optimum particles (Abdelhalim and Habib, 2009; Saed and Kadir, 2011).

4. Results and discussion

4.1. Description of model, PTC specification and climate condition

This system is located in Tehran (capital of Iran) at longitude $+52.5°$ and latitude $+35.7°$ (Tchanche et al., 2009). Table 2 shows the average air temperature, wind velocity and DNI in Tehran (Tchanche et al., 2009). For this optimization the data of 20th July are considered.

Table 3 shows the specifications of PTC studied in this article (Alfellag, 2014; Forristall, 2003; Kalogirou, 2012; Tzivanidis and Bellos, 2016). One main code is prepared in MATLAB software, one code is written for MOPSO algorithm and one code is written to connect main code to optimization code.

4.2. Validation of model

For validation of the obtained results in this model Ref (Alfellag, 2014) will be considered. The specification of PTC and climate conditions studied in that reference are considered as input data. Fig. 5.4, 5.5, and 5.6 of that reference are considered. In those figures outlet temperature of HTF, heat gain and energy efficiency are

Table 2
The monthly average air temperature, wind velocity and DNI in Tehran.

months	Value		
	Air temperature (°C)	Wind velocity (m/s)	DNI (W/m^2)
Jan	2.8	1.5	136.5
Feb	5.1	2.6	190.0
Mar	9.5	2.4	225.0
Apr	15.1	2.8	280.3
May	21.2	2.7	299.9
Jun	26.2	3.1	316.2
Jul	29.3	2.6	311.9
Aug	28.6	2.9	282.7
Sep	24.4	2.8	243.9
Oct	18	2.3	199.0
Nov	11	2.2	156.1
Dec	5.4	1.5	130.8

Table 3
Specifications of PTC.

No	Parameter	Unit	Value	Ref
1	L	m	4.5	Tzivanidis and Bellos (2016)
2	W	m	2.3	Tzivanidis and Bellos (2016)
3	$D_{inner,absorber}$	m	0.047	Tzivanidis and Bellos (2016)
4	$D_{outer,absorber}$	m	0.051	Tzivanidis and Bellos (2016)
5	$D_{inner,glass}$	m	0.07	Tzivanidis and Bellos (2016)
6	$D_{outer,glass}$	m	0.074	Tzivanidis and Bellos (2016)
7	f	m	0.8	Tzivanidis and Bellos (2016)
8	α	–	0.9	[30]
9	k_{glass}	W /mK	1.04	Forristall (2003)
10	ε_{glass}	–	0.86	Forristall (2003)
11	τ_{glass}	–	0.9	Kalogirou (2012)
12	α_{glass}	–	0.02	Forristall (2003)
13	Mirror reflectively	–	0.94	Alfellag (2014)
14	$\dot{m}$	kg/s	0.08	–
15	T_i	°C	30	–

calculated experimentally and theoretically for various hours on 19th Feb. Table 4 shows the comparison the results of this modeling with experimental data of Ref (Alfellag, 2014).

Maximum errors are about 4–5% at 11:16 and 12:28, when it is the highest solar radiation. The reason for this error is to calculate the difference in heat loss in states of theoretical and experimental.

4.3. Optimization of PTC

For optimization with MOPSO algorithm, the two target functions are considered:

$C_H\left(\$/kWh\right)$, Exergy efficiency (%)

The target is maximization the exergy efficiency and minimization of heat cost. Variables considered in this optimization are shown in Table 5. Table 6 shows the MOPSO algorithm setting data.

The maximum iteration of MOPSO algorithm is about 450, number of particles is equal to 100. The repository size and inertia weight are equal to 100 and 1, respectively. Grid inflection parameter is selected 0.1. Number of grid per each dimension is equal to 10 and leader selection pressure parameter is 4. Extra repository member selection pressure is equal to 2.

Table 5
Variables considered for optimization by MOPSO algorithm.

No.	Variable	Unit	Lowe bound	Upper bound
1	$D_{inner,absorber}$	m	0.04	0.06
2	L	m	4	6
3	W	m	2	4
4	$\dot{m}$	kg/s	0.06	0.2
5	f	m	0.4	1.2
6	$D_{outer,absorber}$	m	$D_{outer,absorber} = D_{inner,absorber} + 0.004$	
7	$D_{inner,glass}$	m	$D_{inner,glass} = 1.49 D_{inner,absorber}$	
8	$D_{outer,glass}$	m	$D_{outer,glass} = D_{inner,glass} + 0.004$	

Table 6
MOPSO algorithm setting data.

Variable	Values
Max iteration	450
Number of Particles	100
Repository size	100
Inertia weight	1

The position and velocity of each particle is updated toward the high or low values of objective function is maximization (exergy efficiency (%) or minimization ($c_H\left(\frac{\$}{kWh}\right)$).

Fig. 4 shows the Pareto front of these two target functions.

It is clear that by increasing exergy efficiency, cost of heat ($C_H\left(\$/kWh\right)$) is decreased and vice versa. So the optimal point is located on the right side of this figure. In this point, exergy efficiency is equal to 29.2% and heat cost is equal to 0.0142 ($\$/kWh$).

It is noticeable that for other systems, based on the system configuration, the Pareto front is ascending. For these cases usually the cost function is increased with increasing of exergy efficiency. In these cases, we should define the scenarios for example minimum cost function with minimum exergy efficiency or maximum exergy efficiency with maximum cost function. The optimum values of variable considered this optimization are shown in Table 7. Table 8 shows the key parameters of system before and after optimization.

As shown in Table 8, energy efficiency is improved from 30.81% to 32.55%, but energy destruction rate is increased from 18895.8 W to 23661.44 W due to increasing heat gain rate (1918 W–3536.7 W) and outlet HTF temperature (35.6 °C–37.1 °C).

4.4. Sensitivity analysis

Fig. 5 shows the variation of heat gain rate by changing the inner diameter of absorber from 0.041 m to 0.06 m. From this figure, it is clear that by increasing the inner diameter of absorber, the heat rate gain is decreased.

Table 4
The comparison the results of this modeling with experimental data of Ref (Alfellag, 2014).

Hour	T_0(°C)			Heat gain (W)			Energy efficiency (%)		
	Model	Exp.	Error (%)	Model	Exp.	Error (%)	Model	Exp.	Error (%)
10:04	35.6	36.5	2.5	384	400	4.0	24.9	26	4.2
11:16	42.7	44.2	4.3	647	683	5.2	27.4	29.0	5.5
12:28	41.8	43.7	4.3	765	810	5.5	27.6	29.0	4.8
13:40	47.1	48.6	3.1	812	850	4.4	28.1	29.5	4.7
16:04	38.9	40.5	3.9	533	560	4.8	26.0	27.1	4

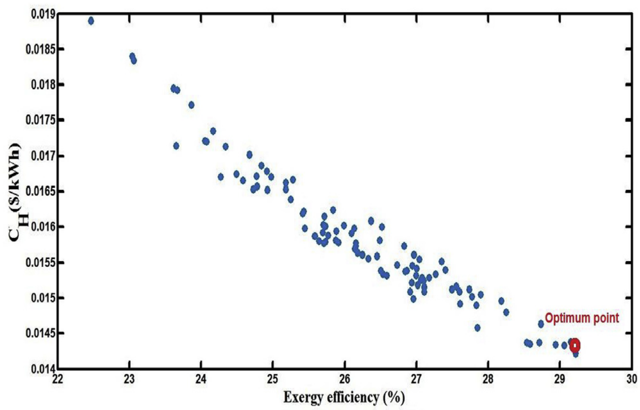

Fig. 4. Pareto front of target functions.

Table 7
The optimum values of variable after optimization.

No	Variable	Unit	Values
1	$D_{inner,absorber}$	m	0.0453
2	L	m	5.55
3	W	m	2.98
4	$\dot{m}$	$kg/_s$	0.115
5	f	m	0.457

Table 8
Key parameters of system before and after optimization.

Variable	Values	
	Before	After
q_u(W)	1918.85	3536.7
T_o (°C)	35.6	37.1
Exergy destruction (W)	18895.8	23661.44
Energy efficiency (%)	30.81	35.55
Exergy efficiency (%)	25.93	29.22
C_H (\$/kWh)	0.0164	0.0142

By increasing the inner diameter of absorber, the three oppose effects can be seen:

1) Increasing the Nusselt number in the absorber. (Positive effect)
2) Decreasing the heat convection coefficient ($h = Nuk/D$) (Negative effect)
3) Increasing the heat transfer from the absorber to glass and surrounding. (Negative effect)

Combining these three effects causes a change in the heat gain rate according to graph shown in Fig. 5. Fig. 6 shows the change in energy efficiency with inner diameter of absorber. By increasing the inner diameter of absorber from 0.041 m to 0.06 m, energy efficiency is decreased from 35.86% to 34.69%. Physical justification of Fig. 6 is similar to Fig. 5.

Fig. 7 shows the variation of exergy destruction with inner diameter of the absorber. Unlike the heat gain rate and energy efficiency, exergy destruction is increased by increasing the inner diameter of absorber. This increase is considerable. By increasing the inner diameter of absorber from 0.041 m to 0.06 m, exergy destruction is increased from 139.55 W to 2719.9 W. Since, regarding to Fig. 7, heat gain rate is decreased by increasing inner diameter, so heat losses as well as exergy destruction are increased.

The variation of heat gain rate and outlet temperature with

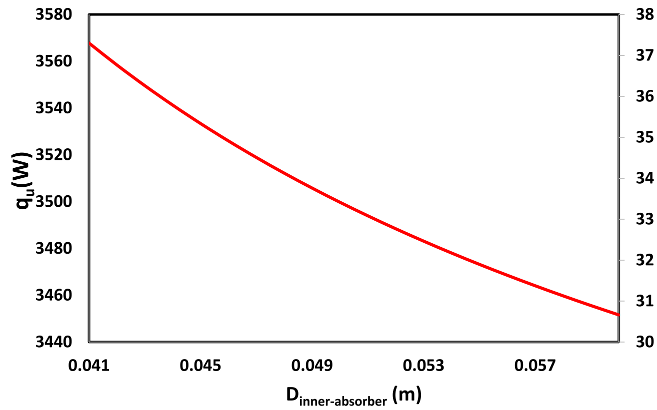

Fig. 5. Variation in heat gain rate by PTC with inner absorber diameter.

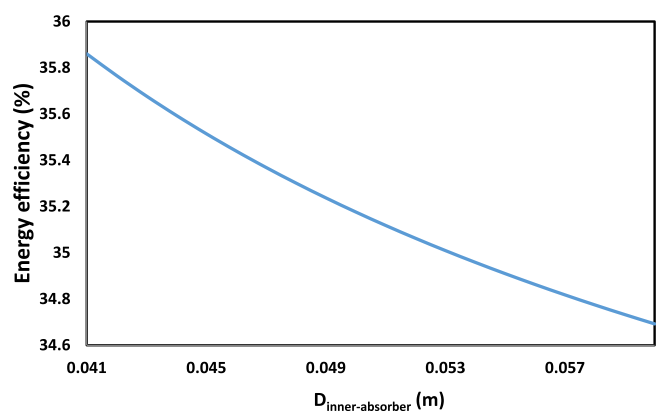

Fig. 6. Changes in energy efficiency with inner diameter of absorber.

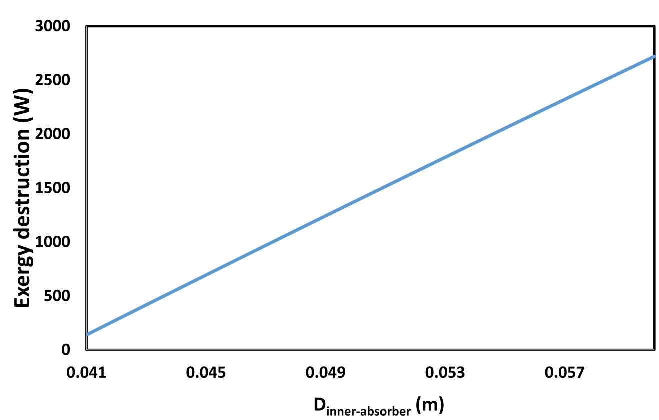

Fig. 7. The variation of exergy destruction with inner diameter of absorber.

length of PTC is shown in Fig. 8. It is clear that, by increasing the length of PTC, heat rate gains and outlet temperature of HTF are increased. In general, by increasing the length of PTC, considering equation (12), outlet temperature of PTC is increased. Also due to equation (18), heat gain rate is increased too.

Fig. 9 shows the variation of energy efficiency with the length of PTC. Similar to Fig. 8, by increasing the length of PTC, energy efficiency is increased.

By increasing the length of PTC from 4 m to 6 m, energy efficiency is increased from 34.1% to 35.8% which this promotion is equal to 5%. This increase in lower than increase in heat gain rate by PTC (57%).

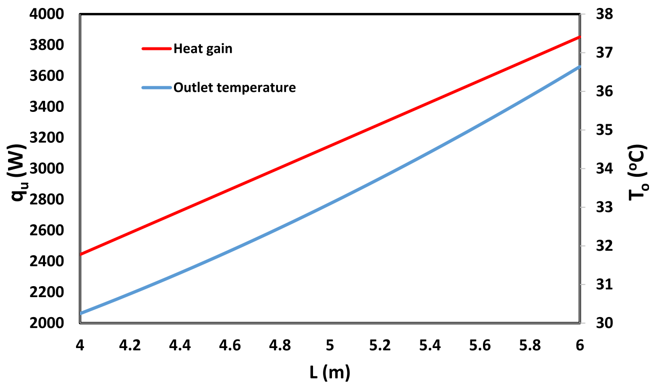

Fig. 8. The variation of heat gains rate and outlet temperature with length of PTC.

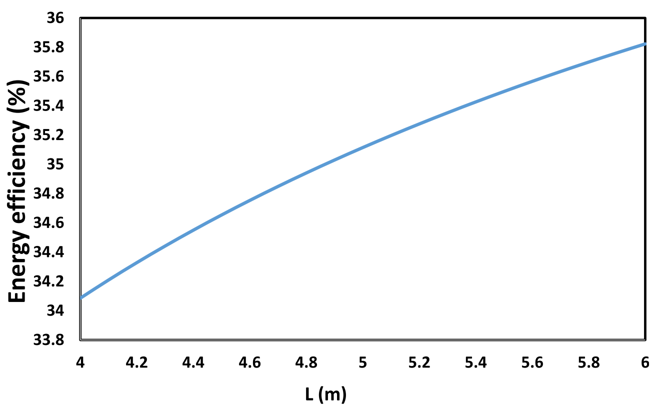

Fig. 9. The variation of energy efficiency versus length of PTC.

The reason is that regarding to equation (17), by increasing the length of PTC, the denominator of this equation is increased too. So the energy efficiency is not increased as much as heat gain rate.

The variation of heat cost with the length of PTC is shown in Fig. 10. By increasing the length of PTC, heat cost is decreased. Since according to denominator of equation (22) and Fig. 8, the denominator of equation (22) is increased so heat cost in decreased although the initial cost of PTC is increased.

Fig. 11 shows the variation of heat gain rate and outlet temperature with the width of PTC.

By increasing the width of PTC from 2 m to 4 m, heat gain rate is increased from 2369 W to 4753.7 W and outlet temperature of HTF

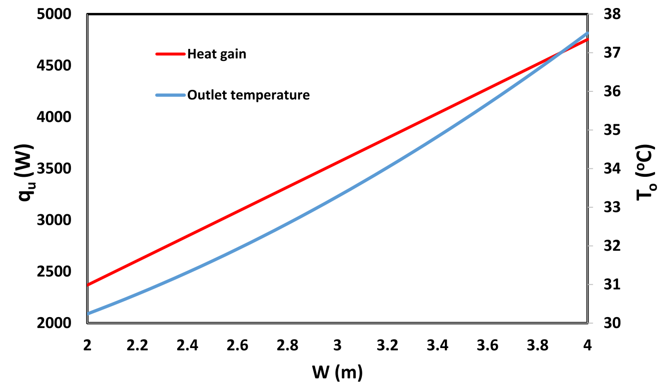

Fig. 11. The variation of heat gain rate and HTF outlet temperature with width of PTC.

is increased for 30.24 °C–37.51 °C. Both increases are considerable.

The effects of width of PTC variation on PTC energy efficiency is shown in Fig. 12. It is clear that increasing the width of PTC does not have a considerable effect on PTC energy efficiency. Since increasing width of PTC from 2 m to 4 m only increases PTC energy efficiency from 35.4% to 35.6%.

So it can be concluded that increasing the length of PTC has more effect on PTC energy efficiency promotion than increasing the width of PTC.

Fig. 13 shows the variation of PTC exergy destruction with width of PTC. It can be seen increasing exergy destruction with the width of PTC is considerable. By increasing the width of PTC from 2 m to 4 m, exergy destruction is increased from 93.71 W to 2873.4 W. Since increasing the width of collector, increases the heat loss from PTC, more than heat gain rate by PTC. So exergy destruction is increased.

Fig. 14 shows the variation of heat rate gained by PTC versus focal length. By increasing the focal length from 0.4 m to 1.2 m, heat gain rate is decreased from 3573.5 W to 2959.2 W. Since considering equations (6) and (7), by increasing the focal length, optical efficiency (η_{opt}) is decreased. So, the heat gain rate in decreased too. It is important to mention that we cannot reduce focal length as much as possible. Since in this case, we have not an appropriate reflection of solar beam.

Fig. 15 shows the variation of PTC energy efficiency with focal length. The effect of focal length on PTC energy efficiency is considerable.

By increasing the focal length from 0.4 m to 1.2 m, energy efficiency is decreased from 35.9% to 29.7%. The variation of exergy destruction with focal length is shown in Fig. 16. The graph is

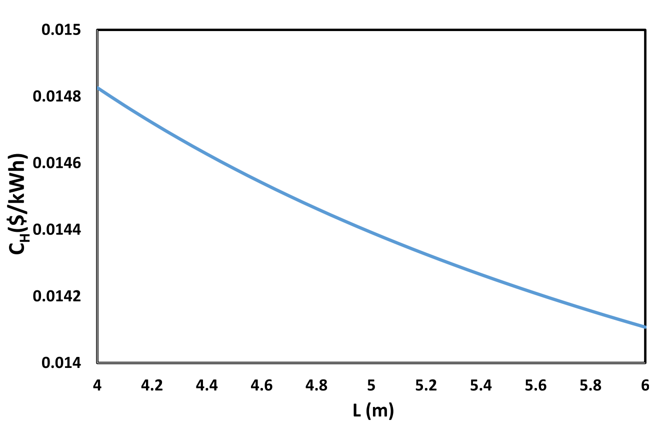

Fig. 10. The variation of heat cost with the length of PTC.

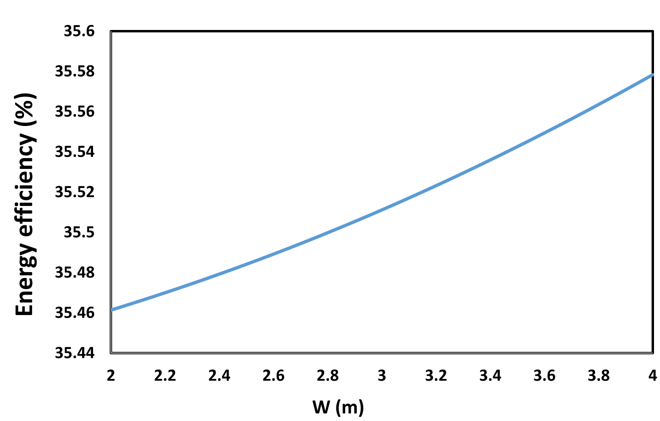

Fig. 12. The variation of PTC energy efficiency with width of PTC.

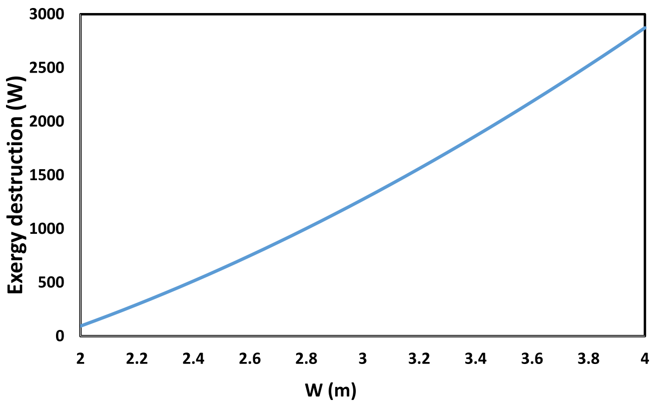

Fig. 13. The variation of exergy destruction of PTC by width of PTC.

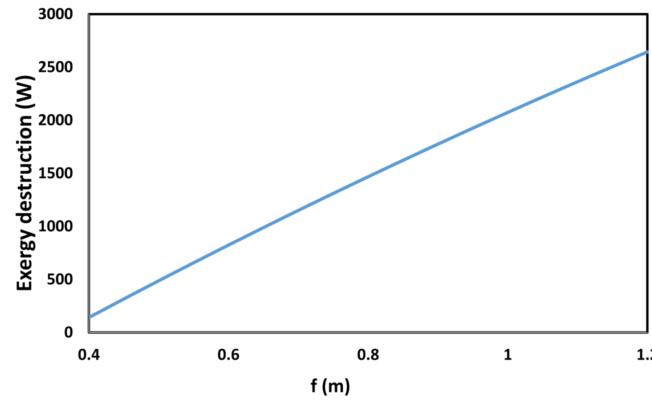

Fig. 16. The variation of exergy destruction with focal length.

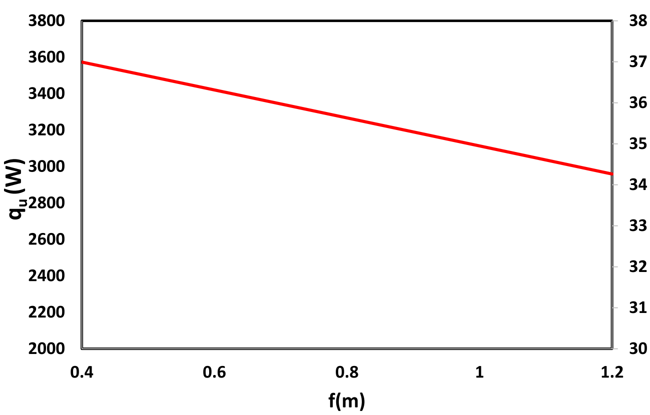

Fig. 14. The variation of heat rate gained by PTC with focal length.

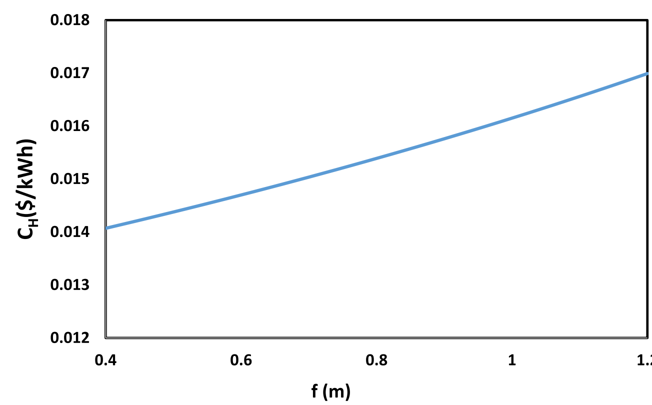

Fig. 17. The variation of cost of heat produced by PTC with focal length.

ascending. It means that by increasing the focal length, exergy destruction is increased.

Fig. 17 shows the variation of cost of heat produced by PTC with focal length. Since heat gain rate in decreased by increasing the focal length, so regarding to equation (27), and the cost of heat is reduced.

Fig. 18 shows the energy efficiency variation with mass flow rate of HTF. By increasing the mass flow rate of HTF, energy efficiency of PTC is increased. In general, by increasing the mass flow rate of HTF, the following oppose effects can be seen.

1) Regarding to equation (13), the Nusselt number and consequently the heat convection coefficient is increased.
2) Regarding to equation (12), the temperature difference in each section is decreased and consequently the outlet temperature of HTF is decreased.

It is clear that point 1 is dominated by point 2, so the heat gain rate and consequently the energy efficiency is increased by increasing mass flow rate of HTF.

4.5. Optimization with another algorithm (multi-objective shuffled frog-leaping algorithm)

Meta-heuristic and evolutionary algorithms are popular algorithms which applied for solving many complex engineering

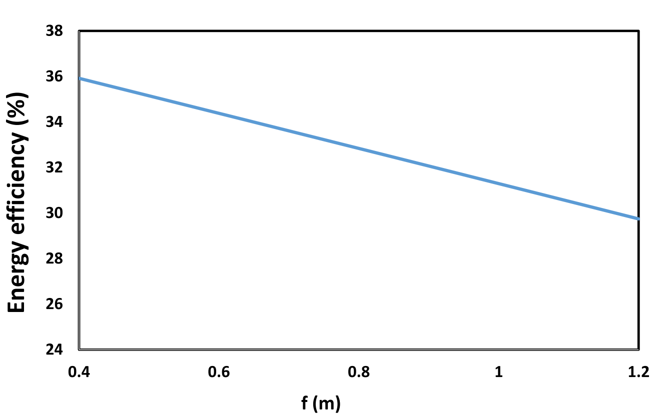

Fig. 15. The variation of PTC energy efficiency with focal length.

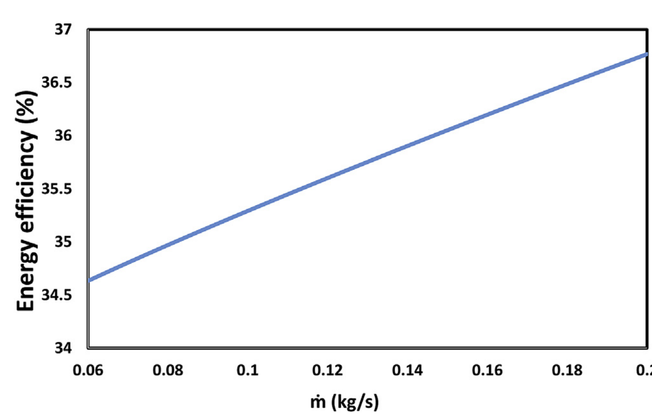

Fig. 18. The energy efficiency variation with HTF mass flow rate.

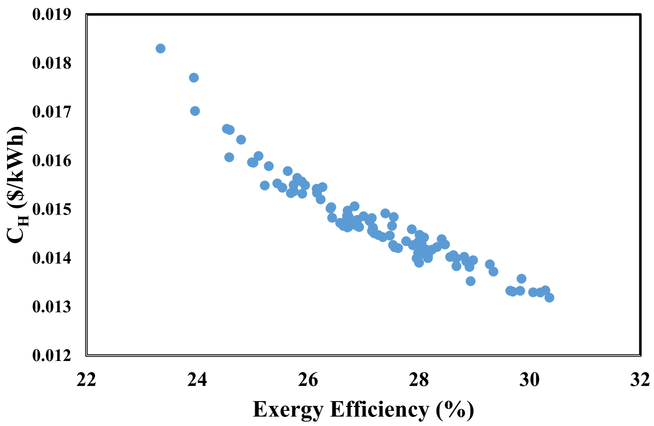

Fig. 19. The Pareto-front curve of optimization by SFLA.

optimization problems (Bozorg-Haddad et al., 2017). The Shuffled Frog-Leaping Algorithm (SFLA) is suggested by Eusuff and Lansey for solving combinatorial optimization problem in 2003.

The SFLA was originally developed as a population-based metaheuristic to perform an informed heuristic search using mathematical functions to find a solution of a combinatorial optimization problem. It combines the benefits of both the genetic-based MA and the social behavior-based PSO algorithm (Rahiminejad et al., 2014). This algorithm performs base on swarm intelligence heuristic computing method that it has a highly effective computing method to find a global optimum based on search method. In shuffled frog leap algorithm (SFLA), the population contains of a set of frogs (solutions) that is partitioned into subsets referred as memeplexes.

The different memeplexes are considered as different cultures of frogs, each performing a local search. In the interior of each memeplex, the individual frogs hold ideas, which can be influenced by the ideas of other frogs, and evolve through a process of memetic evolution. After a defined number of memetic evolution steps, ideas are passed among memeplexes in a shuffling process. The local search and the shuffling processes continue until defined convergence criteria are satisfied (Elbeltagi et al., 2005).

The initial version of this algorithm has some benefits such as simple steps, fast speed, easy concept and few parameters are involved. Nevertheless, some disadvantages are non-uniform initial population, slow convergent rate, limitations in local searching ability and adaptive ability (Jiang et al., 2013; Yuvaraj et al.). The shuffled frog leap algorithm (SFLA) consist of three phases of initialization, evaluation and shuffling which is described in Fig. 18 (Li et al., 2012).

Fig. 19 shows the Pareto-front curve of PTC system by SFLA. By using this algorithm, the exergy efficiency increases to 30.35% (MOPSO 29.22%) and cost of heat decreases to 0.0131 $/kWh (MOPSO 0.0142 $/kWh). Tables 9 and 10 show the values of decision variables and key parameter after optimization by SLFA, respcetively.

Table 9
The optimum values of variable after optimization with shuffled frog-leaping algorithm.

No	Variable	Unit	Values
1	$D_{inner,absorber}$	m	0.0510
2	L	m	4.84
3	W	m	3.22
4	$\dot{m}$	kg/s	0.54
5	f	m	0.1075

Table 10
Key parameters of system before and after optimization with shuffled frog-leaping algorithm.

Variable	Values	
	Before	After
q_u(W)	1918.85	3617.15
T_o (°C)	35.6	38.4
Exergy destruction (W)	18895.8	24112.13
Energy efficiency (%)	30.81	36.62
Exergy efficiency (%)	25.93	30.35
C_H ($/kWh)	0.0164	0.0132

5. Conclusions

Energy production in terms of electricity or heat is a challenging task that needs to be considered when designing a system for that purpose. Moreover, implementing renewable energy source for that purpose makes the task more complex due to the dependence of renewable energy source on weather conditions. Parabolic trough solar collectors are efficient energy convertors for producing steam or hot water. In this work, a PTC located in Tehran is under investigation. Two main factors are the objective of this study namely exergy efficiency and energy cost of PTC. Multiobjective swarm optimization (MOPSO) is coupled with energy, exergy and economic analyses to determine the best possible performance of PTC with minimum energy cost. Three combined computer codes were written for the optimization process. The maximum efficiency was obtained as 29.22% and the minimum energy production cost was about 0.0142 $/kWh. The results of the present model showed good agreement via comparing the energy efficiency with the experimental one available in literature. The absorber inner diameter, length width and focal length of PTC had a considerable influence on PTC performance and energy cost.

Nomenclature:

a	Constant ($\frac{W}{m^2}$)
A	Collector area (m^2)
b	Constant ($\frac{W}{m^2}$)
b	Interaction coefficient
C	Constant ($\frac{W}{m^2}$)
C	Cost of heat produced by PTC ($)
c_p	Constant pressure specific heat ($\frac{kJ}{kg\ K}$)
D	Diameter (m)
DNI	Direct normal irradiance (W)
L	Length of collector (m)
L_{loc}	Location longitude (Degree)
L_{st}	Standard meridian of local zone time (Degree)
$\dot{m}$	Mass flow rate (kg/s)
Nu_D	Nusselt number
Pr	Prandtl number
ex	Specific exergy (J/kg)
f	Friction factor
f	Focal length (m)
h	Convection heat transfer coefficient (W/m^2K)
h	Enthalpy (kJ/kg)
i	Interest rate
K	Incident angle modifier
k	Thermal conductivity $\left(\frac{W}{mK}\right)$
L	Length of collector (m)
$\dot{q}_u$	Useful heat rate gain (W)
$\dot{q}'_1$	Heat convection transfer rate between internal absorber and heat transfer fluid per length ($\frac{W}{m}$)

$\dot{q}'_2$	Heat conduction transfer rate through absorber per length ($\frac{W}{m}$)
$\dot{q}'_3$	Heat convection transfer rate between outer absorber and inner glass per length ($\frac{W}{m}$)
$\dot{q}'_4$	Heat Radiation transfer rate between outer absorber and inner glass per length ($\frac{W}{m}$)
$\dot{q}'_5$	Heat conduction transfer rate through glass per length ($\frac{W}{m}$)
$\dot{q}'_6$	Solar irradiance absorbed by glass per length ($\frac{W}{m}$)
$\dot{q}'_7$	Solar irradiance absorbed by absorbed per length ($\frac{W}{m}$)
$\dot{q}'_8$	Convection heat transfer rate between outer glass and air per length ($\frac{W}{m}$)
$\dot{q}'_9$	Radiation heat trans per rate between outer glass and sky per length ($\frac{W}{m}$)
Re	Reynolds number
s	Specific entropy (kJ/kgK)
T	Temperature (°C)
$\dot{m}$	Mass flow rate ($\frac{kg}{s}$)
W	Width of a collector (m)

Greek Symbols

φ	Latitude (Degree)
δ	Deflection angle ((Degree)
ω	Day time
θ_Z	Zenith Angle (Degree)
ρ	Mirror reflectance factor
ρ	Density $\left(\frac{kg}{m^3}\right)$
τ	Transmittance of glass surrounded the absorber
α	Absorbance factor of a absorber
γ	Intercept factor
L′	End loss factor
ΔL	Length of segment (m)
λ	Mean free path of collisions of molecule (m)
σ	Stefan- Boltzmann constant
μ	Dynamic viscosity $\left(\frac{Ns}{m^2}\right)$

Subscripts

0	Dead state
amb	Ambient
bf	Base fluid
h	Heat
i	Inlet
I	Initial cost
loc	Local time
o	Outlet
OM	Operation and maintenance cost
st	Solar time
w	Wall

References

Ab Wahab, M.N., Nefti-Meziani, S., Atyabi, A., 2015. A comprehensive review of swarm optimization algorithms. PLoS One 10 (5), e0122827.
Abdelhalim, M., Habib, S., 2009. Particle swarm optimization for HW/SW partitioning. Particle Swarm Opt. 49–76.
Alfellag, M.A.A., 2014. Modeling and Experimental Investigation of Parabolic Trough Solar Collector.
Alvarez-Benitez, J.E., Everson, R.M., Fieldsend, J.E., 2005. A MOPSO Algorithm Based Exclusively on Pareto Dominance Concepts, International Conference on Evolutionary Multi-Criterion Optimization. Springer, pp. 459–473.
Aravindan, S., N.G.a.B.A.S, 2018. The recent trends in optimization of thermal performance of parabolic trough solar collector. Int. J. Mech. Eng. Technol. 9 (5), 655–661.
Asgari, E., Ehyaei, M., 2015. Exergy analysis and optimisation of a wind turbine using genetic and searching algorithms. Int. J. Exergy 16 (3), 293–314.
Bejan, A., 2016. Advanced Engineering Thermodynamics. John Wiley & Sons.
Bergman, T.L., Incropera, F.P., DeWitt, D.P., Lavine, A.S., 2011. Fundamentals of Heat and Mass Transfer. John Wiley & Sons.
Boukelia, T., Mecibah, M., Kumar, B., Reddy, K., 2015. Optimization, selection and feasibility study of solar parabolic trough power plants for Algerian conditions. Energy Convers. Manag. 101, 450–459.
Boukelia, T., Arslan, O., Mecibah, M., 2016. ANN-based optimization of a parabolic trough solar thermal power plant. Appl. Therm. Eng. 107, 1210–1218.
Boukelia, T., Arslan, O., Mecibah, M., 2017. Potential assessment of a parabolic trough solar thermal power plant considering hourly analysis: ANN-based approach. Renew. Energy 105, 324–333.
Bozorg-Haddad, O., Solgi, M., Loaiciga, H.A., 2017. Meta-heuristic and Evolutionary Algorithms for Engineering Optimization. John Wiley & Sons.
Coccia, G., Latini, G., Sotte, M., 2012. Mathematical modeling of a prototype of parabolic trough solar collector. J. Renew. Sustain. Energy 4 (2), 023110.
DASHENG, L., 2009. Multi Objective Particle Swarm Optimization: Algorithms and Applications.
Duffie, J.A., 1991. Solar Engineering of Thermal Processes. John A. Duffie, William A. Beckman. Wiley, New York.
Ehyaei, M., Rosen, M.A., 2019. Optimization of a triple cycle based on a solid oxide fuel cell and gas and steam cycles with a multiobjective genetic algorithm and energy, exergy and economic analyses. Energy Convers. Manag. 180, 689–708.
Ehyaei, M.A., Ahmadi, A., Assad, M.E.H., Hachicha, A.A., Said, Z., 2019. Energy, exergy and economic analyses for the selection of working fluid and metal oxide nanofluids in a parabolic trough collector. Sol. Energy 187, 175–184.
El-Gammal, A.A., El-Samahy, A.A., 2009. Adaptive tuning of a PID speed controller for DC motor drives using multi-objective particle swarm optimization. In: 2009 11th International Conference on Computer Modelling and Simulation. IEEE, pp. 398–404.
Elbeltagi, E., Hegazy, T., Grierson, D., 2005. Comparison among five evolutionary-based optimization algorithms. Adv. Eng. Inf. 19 (1), 43–53.
Fernández-García, A., Zarza, E., Valenzuela, L., Pérez, M., 2010. Parabolic-trough solar collectors and their applications. Renew. Sustain. Energy Rev. 14 (7), 1695–1721.
Forristall, R., 2003. Heat Transfer Analysis and Modeling of a Parabolic Trough Solar Receiver Implemented in Engineering Equation Solver. National Renewable Energy Lab., Golden, CO.(US).
Frangopoulos, C.A., 1987. Thermo-economic functional analysis and optimization. Energy 12 (7), 563–571.
Fuqiang, W., Ziming, C., Jianyu, T., Yuan, Y., Yong, S., Linhua, L., 2017. Progress in concentrated solar power technology with parabolic trough collector system: a comprehensive review. Renew. Sustain. Energy Rev. 79, 1314–1328.
Ghasemian, E., Ehyaei, M., 2018. Evaluation and optimization of organic Rankine cycle (ORC) with algorithms NSGA-II, MOPSO, and MOEA for eight coolant fluids. Int. J. Energy Environ. Eng. 9 (1), 39–57.
Gnielinski, V., 1976. New equations for heat and mass transfer in turbulent pipe and channel flow. Int. Chem. Eng. 16 (2), 359–368.
Guo, J., Huai, X., 2016. Multi-parameter optimization design of parabolic trough solar receiver. Appl. Therm. Eng. 98, 73–79.
Güven, H.M., Bannerot, R.B., 1986. Determination of error tolerances for the optical design of parabolic troughs for developing countries. Sol. Energy 36 (6), 535–550.
Hachicha, A., Rodríguez, I., Capdevila, R., Oliva, A., 2013. Heat transfer analysis and numerical simulation of a parabolic trough solar collector. Appl. Energy 111, 581–592.
Han, H.-G., Zhang, L., Qiao, J.-F., 2018. A Gradient Multiobjective Particle Swarm Optimization, Optimization Algorithms-Examples. IntechOpen.
Hojjati, A., Monadi, M., Faridhosseini, A., Mohammadi, M., 2018. Application and comparison of NSGA-II and MOPSO in multi-objective optimization of water resources systems. J. Hydrol. Hydromechanics 66 (3), 323–329.
Horngren, C.T., Foster, G., Datar, S.M., Rajan, M., Ittner, C., Baldwin, A.A., 2010. Cost accounting: a managerial emphasis. Issues Account. Educ. 25 (4), 789–790.
Hosseini, S.S., Hamidi, S.A., Mansuri, M., Ghoddosian, A., 2015. Multi Objective Particle Swarm Optimization (MOPSO) for size and shape optimization of 2D truss structures. Period. Polytech. Civ. Eng. 59 (1), 9–14.
Jebasingh, V., Herbert, G.J., 2016. A review of solar parabolic trough collector. Renew. Sustain. Energy Rev. 54, 1085–1091.
Jiang, J., Ma, P., Gao, X., Li, J., Zhao, F., 2013. An improved shuffled Frog Leaping algorithm. J. Inf. Comput. Sci. 10 (6), 1665–1673.
Kalogirou, S.A., 2012. A detailed thermal model of a parabolic trough collector receiver. Energy 48 (1), 298–306.
Khaled, A., 2012. Technical and Economic Performance of Parabolic Trough in Jordan. Amman (Jordan).
Kulkarni, V.R., Desai, V., 2016. ABC and PSO: A Comparative Analysis, 2016 IEEE International Conference on Computational Intelligence and Computing Research (ICCIC). IEEE, pp. 1–7.
Kusiak, A., Xu, G., 2012. Modeling and optimization of HVAC systems using a dynamic neural network. Energy 42 (1), 241–250.
Lalwani, S., Singhal, S., Kumar, R., Gupta, N., 2013. A comprehensive survey: applications of multi-objective particle swarm optimization (MOPSO) algorithm. Trans. Combin. 2 (1), 39–101.
Li, J., Pan, Q., Xie, S., 2012. An effective shuffled frog-leaping algorithm for multi-objective flexible job shop scheduling problems. Appl. Math. Comput. 218 (18), 9353–9371.
Liu, Q., Yang, M., Lei, J., Jin, H., Gao, Z., Wang, Y., 2012. Modeling and optimizing parabolic trough solar collector systems using the least squares support vector

machine method. Sol. Energy 86 (7), 1973–1980.
Montes, M., Abánades, A., Martínez-Val, J., 2009. Performance of a direct steam generation solar thermal power plant for electricity production as a function of the solar multiple. Sol. Energy 83 (5), 679–689.
Montes, M., Abánades, A., Martínez-Val, J., Valdés, M., 2009. Solar multiple optimization for a solar-only thermal power plant, using oil as heat transfer fluid in the parabolic trough collectors. Sol. Energy 83 (12), 2165–2176.
Okonkwo, E.C., Abid, M., Ratlamwala, T.A., 2018. Numerical analysis of heat transfer enhancement in a parabolic trough collector based on geometry modifications and working fluid usage. J. Sol. Energy Eng. 140 (5), 051009.
Padilla, R.V., Fontalvo, A., Demirkaya, G., Martinez, A., Quiroga, A.G., 2014. Exergy analysis of parabolic trough solar receiver. Appl. Therm. Eng. 67 (1–2), 579–586.
Palenzuela, P., Alarcón-Padilla, D.-C., Zaragoza, G., 2015. Large-scale solar desalination by combination with CSP: techno-economic analysis of different options for the Mediterranean Sea and the Arabian Gulf. Desalination 366, 130–138.
Petela, R., 1964. Exergy of heat radiation. J. Heat Transf. 86 (2), 187–192.
Rahiminejad, A., Alimardani, A., Vahidi, B., Hosseinian, S.H., 2014. Shuffled frog leaping algorithm optimization for AC–DC optimal power flow dispatch. Turk. J. Electr. Eng. Comput. Sci. 22 (4), 874–892.
Rao, S.S., 2009. Engineering Optimization: Theory and Practice. John Wiley & Sons.
Rathore, M.M., Kapuno, R., 2011. Engineering Heat Transfer. Jones & Bartlett Publishers.
Ratzel, A., Hickox, C., Gartling, D., 1979. Techniques for reducing thermal conduction and natural convection heat losses in annular receiver geometries. J. Heat Transf. 101 (1), 108–113.
Reyes-Sierra, M., Coello, C.C., 2006. Multi-objective particle swarm optimizers: a survey of the state-of-the-art. Int. J. Comput. Intell. Res. 2 (3), 287–308.
Sadeghzadeh, H., Aliehyaei, M., Rosen, M., 2015. Optimization of a Finned shell and tube heat exchanger using a multi-objective optimization genetic algorithm. Sustainability 7 (9), 11679–11695.
Sadeghzadeh, H., Ehyaei, M., Rosen, M., 2015. Techno-economic optimization of a shell and tube heat exchanger by genetic and particle swarm algorithms. Energy Convers. Manag. 93, 84–91.
Saed, A.A., Kadir, W.M.W., 2011. Applying Particle Swarm Optimization to Software Performance Prediction an Introduction to the Approach, 2011 Malaysian Conference in Software Engineering. IEEE, pp. 207–212.
Shamoushaki, M., Ehyaei, M., Ghanatir, F., 2017. Exergy, economic and environmental analysis and multi-objective optimization of a SOFC-GT power plant. Energy 134, 515–531.
Shamoushaki, M., Ghanatir, F., Ehyaei, M., Ahmadi, A., 2017. Exergy and exergoeconomic analysis and multi-objective optimisation of gas turbine power plant by evolutionary algorithms. Case study: aliabad Katoul power plant. Int. J. Exergy 22 (3), 279–307.
Shirmohammadi, R., Ghorbani, B., Hamedi, M., Hamedi, M.-H., Romeo, L.M., 2015. Optimization of mixed refrigerant systems in low temperature applications by means of group method of data handling (GMDH). J. Nat. Gas Sci. Eng. 26, 303–312.
Silva, R., Berenguel, M., Pérez, M., Fernández-Garcia, A., 2014. Thermo-economic design optimization of parabolic trough solar plants for industrial process heat applications with memetic algorithms. Appl. Energy 113, 603–614.
Silveira, J., Tuna, C., 2003. Thermoeconomic analysis method for optimization of combined heat and power systems. Part I. Prog. Energy Combust. Sci. 29 (6), 479–485.
Sukhatme, K., Sukhatme, S.P., 1996. Solar Energy: Principles of Thermal Collection and Storage. Tata McGraw-Hill Education.
Tarique, A., Gabbar, H.A., 2013. Particle swarm optimization (PSO) based turbine control. Intell. Control Autom. 4 (02), 126.
Tchanche, B., Papadakis, G., Lambrinos, G., Frangoudakis, A., 2009. Fluid Selection for a Low-Temperature Solar Organic Rankine Cycle.
Tripathi, P.K., Bandyopadhyay, S., Pal, S.K., 2007. Multi-objective particle swarm optimization with time variant inertia and acceleration coefficients. Inf. Sci. 177 (22), 5033–5049.
Tzivanidis, C., Bellos, E., 2016. The use of parabolic trough collectors for solar cooling – a case study for Athens climate. Case Stud. Ther. Eng. 8, 403–413.
Vasquez Padilla, R., 2011. Simplified Methodology for Designing Parabolic Trough Solar Power Plants.
Yazdi, B.A., Yazdi, B.A., Ehyaei, M.A., Ahmadi, A., 2015. Optimization of micro combined heat and power gas turbine by genetic algorithm. Therm. Sci. 19 (1), 207–218.
Yousefi, M., Ehyaei, M., 2017. Feasibility study of using organic Rankine and reciprocating engine systems for supplying demand loads of a residential building. Adv. Build. Energy Res. 1–17.
Yunus, C.A., Afshin, J.G., 2011. Heat and Mass Transfer: Fundamentals and Applications. Tata McGraw-Hill, New Delhi, India.
Yuvaraj, N., SriPreethaa, K., Kathiresan, K., Extensive Survey on Datamining Algoritms for Pattern Extraction.
Zadeh, P.M., Sokhansefat, T., Kasaeian, A., Kowsary, F., Akbarzadeh, A., 2015. Hybrid optimization algorithm for thermal analysis in a solar parabolic trough collector based on nanofluid. Energy 82, 857–864.